COPY RIGHT

ELSEVIER SSRN

Title: A NOVEL METHOD OF NEW MULTI-INPUT DC-DC CONVERTER FOR HYBRID ELECTRIC VEHICLES

Paper Authors

HARITHA KALYANAM, S M GAVASKAR MEDABALIMI

st mary engineering college chebrolu, andhra Pradesh

.

USE THIS BARCODE TO ACCESS YOUR ONLINE PAPER

To Secure Your Paper As Per UGC Guidelines We Are Providing A Electronic Bar Code

A NOVEL METHOD OF NEW MULTI-INPUT DC-DC CONVERTER FOR HYBRID ELECTRIC VEHICLES

[1]HARITHA KALYANAM, [2]S M GAVASKAR MEDABALIMI

[1]M-Tech Student Scholar, Department of Power Electronics and Electrical Drives, st mary engineering college chebrolu, Andhra Pradesh

[2]Head of the Department and Professor, Department of Power Electronics and Electrical Drives, st mary, engineering college chebrolu, A.P

[1]harithakalyanam220@gmail.com,[2]gavaskar267@gmail. Com

ABSTRACT: This project proposes a new multi-input isolated DC-DC converter for hybrid electric vehicles application. In this work, fuel cell and energy storage system are utilized as the input sources for the proposed system. Fuel is considered as the main power supply. Utilized to charge the battery, increase the efficiency, reduce fuel economy and supplying the output load ,charging and discharging the battery can be made by the FC and pv sources simultaneously or individually. The main advantage of proposed converter is that, the proposed multi input converter has a capability of providing the demanded power by load in absence of one or two resources.

I. INTRODUCTION

Due to increasing diligence on energy crisis and environmental protection, the Hybrid Electric Vehicles (HEVS) arereceived lot of attention in recent years. Petroleum is used world-wide at a higher rate due to the wider requirement oftransport. It plays a major role in modelling the vehicles with minimum and without consumption of petroleum. Andtherefore the alternate propulsion technologies have been increasingly engaged by the automobile industries and thishassled to the increased exploitation rate of HEV. One of the main advantages for the HEV drive is to improve theefficiency of the motor drive. The key components of the traction systems in hybrid electric vehicles are the multi inputbidirectional DC-DC converters. Multi input bidirectional converters have combine the different sources, such asbatteries, ultra capacitor, photovoltaic cells, fuel cells, and other renewable energy sources, with different voltagecharacteristics.The designs characteristic of the induction motor are used in HEV (1-6), the overview of HEV are discussed. Byapplying suitable starting frequency and voltage for the inverter fed induction motor low starting current and highstarting torque can be obtained (7). Using high frequency transformer to connect different sources, where each sourceis connected by full-bridge cells using 12 switches for three sources (8). A current fed half-bridge topology has beenproposed in [9] to reduce the ripple current in the battery using phase shift modulation. The stability analyses ofmultiple input isolated buck–boost and forward converters along have been presented in [10]. In these types ofconverters, power sharing between various sources is difficult to control. In

[11], energy flow between number ofdifferent sources and the dc link are discussed. In this topology, it is not possible to transfer energy directly between dcsources, and also, a higher number of devices are being used.In this paper a new type of multi input bidirectional DCDC converter will be proposed in order to integrate various energy sources. The proposed circuit will beanalyzed, modelled, designed, controlled, and simulated. Due to the advantages like low cost and compact structuremulti input bidirectional DC-DC converter are reported to be designed for HEV application.DC-DC converter is an electrical circuit which provides varying voltage levels that differs from the supplied voltage.DC-DC converter is employed in variety of application. The unregulated DC voltage is given as the input to the DCDC converter. That converter produces the regulated output voltage even though the input voltage is changing. Due to the fact that initial cost of PVs is high and in order to increase the extracted power from the PV panels, MPPTalgorithm has to be utilized. In [22], a general comparison is made between different MPPT techniques with respect to tracking factor, dynamic response, PV voltage ripple, and use of sensors. The other way to improve the efficiency is to enhance the efficiency of the electric components [23].
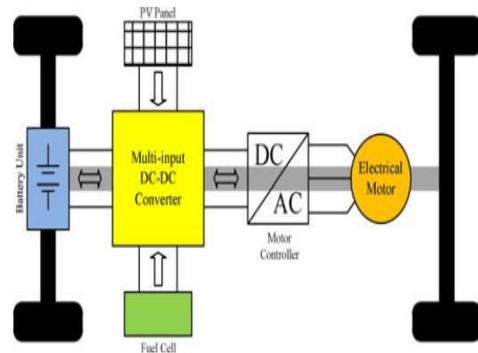

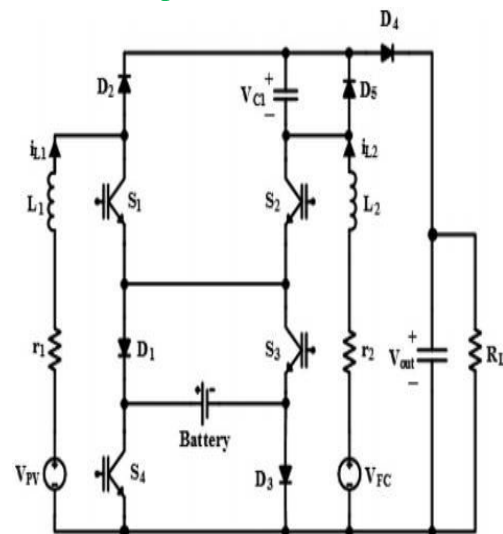Fig. 1. General structure of the multi powered HEV.

Fig. 2. Three-input dc–dc boost converter.

In this study, a novel three-input dc–dc converter is proposed to merge a PV, a fuel cell, and a battery and connect them to the grid. Furthermore, dc gain is enhanced in respect of conventional converters. Meanwhile, MPPT can be obtained for PV. The battery can be charged and discharged in order to achieve power management. In the following two sections, the proposed structure is studied and different operation modes are discussed.

II PROPOSED CONVERTER TOPOLOGY

The structure of the proposed three-input dc–dc boost converter is depicted in Fig. 2. The converter is formed of two conventional boost converters, substituting

International Journal for Innovative Engineering and Management Research
PEER REVIEWED OPEN ACCESS INTERNATIONAL JOURNAL
www.ijiemr.org

extra capacitor in one of the converters, and a battery to store the energy. Characteristic of the converter is suitable for hybrid systems. In this paper, behavior of the converter in terms of managing the sources is analyzed in power management and control part. Then, v_{PV} and v_{FC} are two independent power sources that output is based on characteristic of them. L1 and L2 are the inductances of input filters of PV panel and fuel cell. Using L1 and L2 as in series with input sources change PV and FC modules to current sources. r1 and r2 are vPV 'S and vF C 'S equivalent resistance, respectively. RLoad is the equivalent resistance of loads connected to the dc bus. S1, S2, S3, and S4 are power switches.Diodes D1, D2, D3, and D4 are used to establish modes, which will be described. Capacitor C1 is used to increase output gain and output capacitor Co is performed as an output voltage filter. System is operating in continuous-conduct mode to produce smooth current with least possible amount of current ripple.

III OPERATION MODES

In this section, principles of the proposed converter are discussed. Operation of the converter is divided into three states:

1) The load is supplied by PV and FC and battery is not used.

2) The load is supplied by PV, FC, and battery, in this state, battery is in discharging mode.

3) The load is supplied by PV and FC and battery is in charging mode.

A First Operation State (the Load is Supplied by PV and FC While Battery is Not Used)

In this state, as it is illustrated in Fig. 3, there are three operation modes. During this state, the system is operating without battery charging or discharging. Therefore, there are two paths for current to flow

(through S3 and D3 or D1 and S4). In this paper, S3 and D3 is considered as common path. However, D1 and S4 could be chosen as an alternative path. During this state, switch S3 is permanently ON and switch S4 is OFF.

Mode 1: (0 < t < d1T): In this interval, switches S1, S2, S3, and diode D3 are turned ON. Inductors L1 and L2 are charged via power sources VPV and VF C , respectively [see Fig. 3(a)].

Mode 2: (d1T < t < d2T): In this interval, switch S1 is turned OFF and D2 is turned ON and S2, S3, and D3 are still ON. Inductor L2 is still charged and inductor L1 is being discharged via VPC − VF C [see Fig. 3(b)].

Mode 3: (d2T < t < T): In this interval, S1 is turned ON and S2 is turned OFF and S3 and D3 are still ON. Inductor L1 is charged with VPV and inductor L2 is discharged via VPV + VC 1 − Vo[see Fig. 3(c)].

By applying the voltage–second balance low over the inductors L1 and L2, voltage of capacitor C1 and output voltage can be obtained as follows:

$$L_1 : d_1 \left[V_{PV} - r_1 i_{L_1} \right] + (d_2 - d_1) \left[V_{PV} - r_1 i_{L_1} - V_{C_1} \right]$$
$$+ (1 - d_2) \left[V_{PV} - r_1 i_{L_1} \right] = 0$$

$$(1)$$

$$V_{C_1} = \frac{V_{PV} - r_1 i_{L_1}}{d_2 - d_1}$$

$$(2)$$

$$L_2 : d_2 \left[V_{FC} - r_2 i_{L_2} \right] + (1 - d_2) \left[V_{FC} + V_{C_1} - r_2 i_{L_2} - V_o \right] = 0$$

$$(3)$$

$$V_o = \frac{(d_2 - d_1) \left(V_{FC} - r_2 i_{L_2} \right) + (1 - d_2) \left(V_{FC} - r_1 i_{L_1} \right)}{(1 - d_2)(d_2 - d_1)}.$$
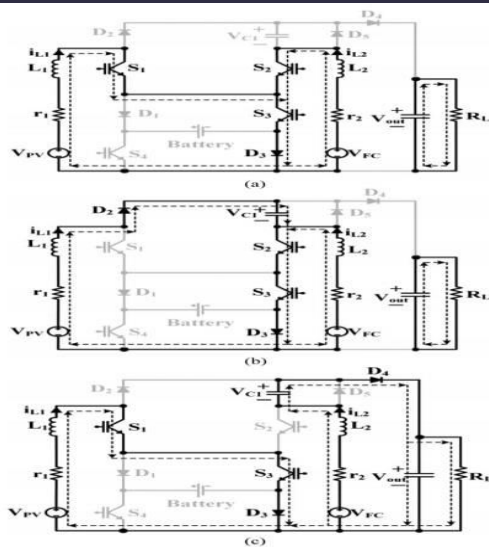
$$(4)$$

Fig. 4.3. Current-flow path of operating modes in first operating state. (a) Mode 1. (b) Mode 2. (c) Mode 3.

Also, by applying the current–second balance low over the capacitors C1 and Co, voltage of capacitor C1, we have

$$C_1 : (d_2 - d_1) i_{L_1} - (1 - d_2) i_{L_2} = 0 \tag{5}$$

$$C_0 : (1 - d_2) i_{L_2} = \frac{V_o}{R_{\text{Load}}}. \tag{6}$$

In this case, battery is not used and so we have

$$i_{\text{batt}} = 0$$

$$P_{\text{batt}} = 0. \tag{7}$$

B. Second Operation State (the Load is Supplied by PV, FC, and Battery)

In this state, as it is illustrated in Fig. 4, there are four operation modes. During this state, the load is supplied by all input sources (PV, FC, and battery). In first mode, there is only one current path. However, in other three modes, there are two current paths (through S3 and D3 or D1 and S4). In this state, current flows through D1 and S4. Switch S4 is permanently ON during this state.

Mode 1: (0 < t < d1T): In this interval, S1, S2, S3, and S4 are turned ON. Inductors L1 and L2 are charged by VPV + vBattery and VF C + vBattery, respectively [see Fig. 4(a)].

Mode 2: (d1T < t < d2T): In this interval, S1, S2, S4, and D1 are turned ON. Inductors L1 and L2 are charged by VPV and VF C , respectively [see Fig. 4(b)].

Mode 3: (d2 T < t < d3T): In this interval, S2, S4, D1, and D2 are turned ON. Inductor L1 is discharged to capacitor C1 and L2 is charged by vF C [see Fig. 4(c)].

Mode 4: (d3T < t < d4T): In this interval, S1, S4, D1, and D4 are turned ON. Inductor L1 is charged by VPV and inductor L2 discharges C1 to the output capacitor [see Fig. 4(d)].

By applying the voltage–second balance low over the inductors L1 and L2, we have

$$L_1 : d_1 \left[V_{\text{PV}} + V_{\text{batt}} - r_1 i_{L_1} \right] + (d_2 - d_1) \left[V_{\text{PV}} - r_1 i_{L_1} \right]$$
$$+ (d_3 - d_2) \left[V_{\text{PV}} - r_1 i_{L_1} - V_{C_1} \right] + (1 - d_3) \left[V_{\text{PV}} - r_1 i_{L_1} \right] = 0 \tag{8}$$

And then

$$V_{C_1} = \frac{V_{\text{PV}} + d_1 V_{\text{batt}} - r_1 i_{L_1}}{d_3 - d_2}$$
$$\times L_2 : d_1 \left[V_{FC} + V_{\text{batt}} - r_2 i_{L_2} \right] + (d_3 - d_1) \left[V_{FC} - r_2 i_{L_2} \right]$$
$$+ (1 - d_3) \left[V_{FC} + V_{C_1} - r_2 i_{L_2} - V_o \right] = 0. \tag{9}$$

$$V_o =$$
$$\frac{(d_3 - d_2) \left(V_{FC} + d_1 V_{\text{batt}} - r_2 i_{L_2} \right) + (1 - d_3) \left(V_{\text{PV}} + d_1 V_{\text{batt}} - r_1 i_{L_1} \right)}{(1 - d_3)(d_3 - d_2)}. \tag{4.10}$$

Also, by applying the current–second balance low over the capacitors C1 and Co, voltage of capacitor C1, we have

$$C_1 : (d_3 - d_2) i_{L_1} - (1 - d_3) i_{L_2} = 0 \tag{4.11}$$

$$C_o : (1 - d_3) i_{L_2} = \frac{V_o}{R_{\text{Load}}}.$$

(4.12)

In this state, the current and power of battery can be calculated as (4.13) and (4.14), respectively

$$i_{\text{batt}} = d_1 \left(i_{L_2} + i_{L_1} \right)$$

(4.13)

$$P_{\text{batt}} = V_{\text{batt}} \left[d_1 \left(i_{L_2} + i_{L_1} \right) \right].$$

(4.14)

C. Third Operation State (the Load is Supplied by PV and FCWhile Battery is in Charging Mode)

In this state, as it is illustrated in Fig. 5, there are four modes. During this state, PV and FC charges the battery and supply the energy of load.
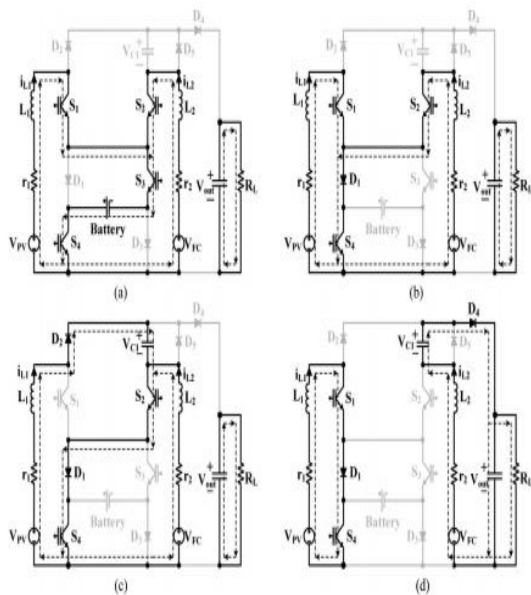
Fig. .4. Current-flow paths in different operation modes of second state. (a) Mode 1. (b) Mode 2. (c) Mode 3. (d) Mode 4.
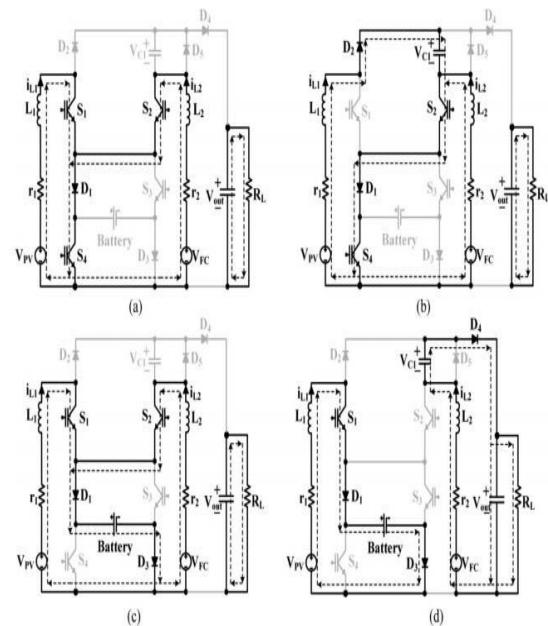
Fig. 5. Current-flow path of operating modes in third operating state. (a) Mode 1. (b) Mode 2. (c) Mode 3. (d) Mode 4.

In the first- and second-operation modes, there are two possible current paths through S3 and D3 or D1 and S4). The path D1 and S4 is chosen to flow the current in this state. During this state, switch S3 is permanently OFF and diode D1 conducts.

Mode 1: ($0 < t < d1T$): In this interval, S1, S2, S4, and D1 are turned ON. Inductors L1 and L2 are charged by vPV and vF C , respectively [see Fig. 4.5(a)].

Mode 2: ($d1T < t < d2T$): In this interval, S2, S4, and D1 are turned ON. Inductor L1 is discharged to capacitor C1 and inductor L2 is charged by vF C [see Fig. 4.5(b)].

Mode 3: ($d2\,T < t < d3\,T$): In this interval, S1, S2, D1, and D3 are turned ON. Inductors L1 and L2 are charged by vPV − vBattery and vF C − vBattery , respectively [see Fig. 4.5(c)].

Mode 4: ($d3\,T < t < d4\,T$): In this interval, S1, S4, D1, and D4 are turned ON. Inductor L1 is charged by vPV − vBattery and inductor L2 is discharged by vF C − vC 1 − vo[see Fig. 4.5(d)].

International Journal for Innovative Engineering and Management Research
PEER REVIEWED OPEN ACCESS INTERNATIONAL JOURNAL
www.ijiemr.org

By applying the voltage–second balance low over the inductors L1 and L2, we have

$$L_1 : d_1 \left[V_{PV} - r_1 i_{L_1} \right] + (d_2 - d_1) \left[V_{PV} - r_1 i_{L_1} - V_{C_1} \right]$$
$$+ (1 - d_2) \left[V_{PV} - r_1 i_{L_1} - V_{batt} \right] = 0$$

(15)

$$V_{C_1} = \frac{V_{PV} - (1 - d_2) V_{batt} - r_1 i_{L_1}}{d_2 - d_1}$$

(16)

$$L_2 : d_2 \left[V_{FC} - r_2 i_{L_2} \right] + (d_3 - d_2) \left[V_{FC} - r_2 i_{L_2} - V_{batt} \right]$$
$$+ (1 - d_3) \left[V_{FC} + V_{C_1} - r_2 i_{L_2} - V_o \right] = 0$$

(17)

$$V_o = \frac{(V_{FC} - (d_3 - d_2) V_{batt} - r_2 i_{L_2})}{(1 - d_3)}$$
$$+ \frac{(V_{PV} - (1 - d_2) V_{batt} - r_1 i_{L_1})}{(d_2 - d_1)}.$$

(18)

By applying current–second balance low to capacitors C1 and Co, we have

$$C_1 : (d_2 - d_1) i_{L_1} - (1 - d_3) i_{L_2} = 0$$

(19)

$$C_o : (1 - d_3) i_{L_2} = \frac{V_o}{R_{Load}}.$$

(20)

In this state, the current and delivered power by battery can be obtained as (4.21) and (4.22)

$$i_{batt} = (d_3 - d_2)(i_{L_2} + i_{L_1}) + (1 - d_3) i_{L_1}$$

(21)

$$P_{batt} = V_{batt} \left[(d_3 - d_2)(i_{L_2} + i_{L_1}) + (1 - d_3) i_{L_1} \right]$$

(22)

Fig..6 illustrates switching pattern for each state and each mode. To fulfill switching operation, a saw-tooth wave as a carrier is compared with signals d1, d2, d3, and d4, which can independently control on state of power switches. Without considering output voltage utilized power of each sources PV, FC, and battery can be controlled using d1, d2, d3, and d4 signals. The voltage gain of the proposed converter is compared with the converter proposed. As shown in this figure, the voltage gain of the proposed converter is higher than the converter proposed in [24]. Benefiting from high-voltage gain, the proposed converter achieve the specific output voltage VO with less duty cycles in comparison with the converter proposed in [24] which increase the efficiency of the proposed converter. It is worth noting that in this figure, the inductor resistances are ignored and the voltage gain is compared in the first operation mode. Input voltages are also considered the same.

IV. DYNAMIC MODELING AND CONTROL

In order to control and analyze dynamic performance of the proposed converter, it should be modeled. As it has been mentioned, the presented converter operates in three states that first state is made of three modes and second and third states are contained of four modes. Each state operates to provide particular goals, which will be explained. In first state, output voltage and only one of the input power sources can be controlled. Due to this fact in this paper, we decide to control PV power source, which can be replaced by FC source as well. In second state because of interference the battery, output voltages and input sources power rate can be controlled. Third states' control parameters due to interference the battery

is same as second state. As mentioned previously interference the battery consists of two states, which in one of them battery will be charged and in one of them battery will be discharged. Selection of proper state (without battery, battery charging, battery discharging) is depends on power managing algorithm. Dynamic model of the proposed converter for each state is as follows.

First state: In this state, d1 and d2 as control variables, control output voltage, and power rate of one of the input sources that is consider PV in this paper. State-space model of converter for first state is

$$L_1 \frac{di_{L1}}{dt} = V_{PV} + (d_1 - d_2) V_{C1} - r_1 i_{L1}$$

(23)

$$L_2 \frac{di_{L2}}{dt} = V_{FC} + (1 - d_2) V_{C1} + (d_2 - 1) V_o - r_2 i_{L2}$$

(24)

$$C_o \frac{dV_o}{dt} = (1 - d_2) i_{L_2} - \frac{V_o}{R_{\text{Load}}}$$

(25)

$$C_1 \frac{dV_{C1}}{dt} = (d_2 - d_1) i_{L1} - (1 - d_2) i_{L2}.$$

(26)

Second state: In this state, three control variables d1, d2, and d3 are used for controlling three state variables. In this state, the state-space model of converter is

$$L_1 \frac{di_{L1}}{dt} = V_{PV} + d_1 V_{\text{batt}} + (d_2 - d_3) V_{C1} - r_1 i_{L1}$$

(27)

$$L_2 \frac{di_{L2}}{dt} = V_{FC} + d_1 V_{\text{batt}} + (1 - d_3) V_{C1} + (d_3 - 1) V_o - r_2 i_{L2}$$

(28)

$$C_o \frac{dV_o}{dt} = (1 - d_3) i_{L_2} - \frac{V_o}{R_{\text{Load}}}$$

(29)

$$C_1 \frac{dV_{C1}}{dt} = (d_3 - d_2) i_{L1} - (1 - d_3) i_{L2}.$$

(30)

Third state: In this state, same as second state, three state variables are controlled by three control variables d1, d2, and d3 controlling. State-space model of the converter in this state can be written as follows:

$$L_1 \frac{di_{L1}}{dt} = V_{PV} + (d_2 - 1) V_{\text{batt}} + (d_1 - d_2) V_{C1} - r_1 i_{L1}$$

(31)

$$L_2 \frac{di_{L2}}{dt} = V_{FC} + (d_2 - d_3) V_{\text{batt}} + (1 - d_3) V_{C1} + (d_3 - 1) V_o - r_2 i_{L2}$$

(32)

$$C_o \frac{dV_o}{dt} = (1 - d_3) i_{L_2} - \frac{V_o}{R_{\text{Load}}}$$

(33)

$$C_1 \frac{dV_{C1}}{dt} = (d_2 - d_1) i_{L1} - (1 - d_3) i_{L2}.$$

(34)

(a)   (b)   (c)
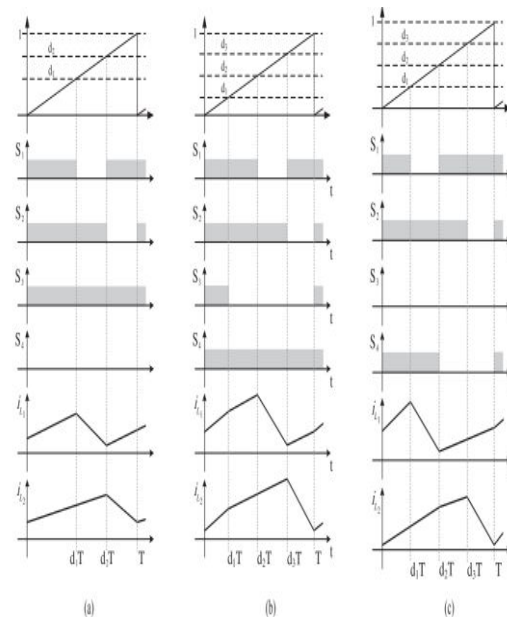
Fig. 6. Switching pattern for three states. (a) First state. (b) Second state. (c) Third state.
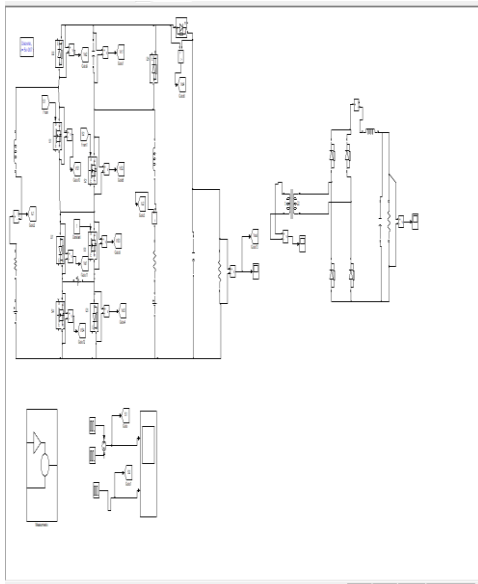
V SIMULATION RESULTS

FIG 7 The load is supplied by PV and FC while battery is not usedFirst operation state
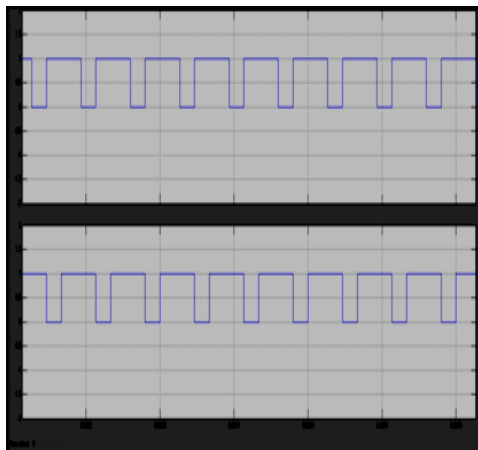
SWITCHES S1 and S2
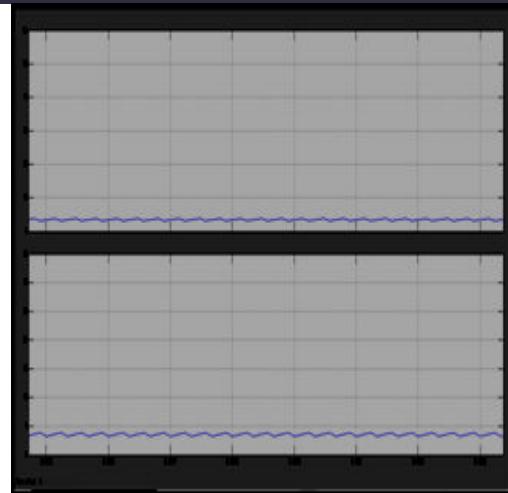

FIG 8 simulations of Switches S1 and S2waveforms
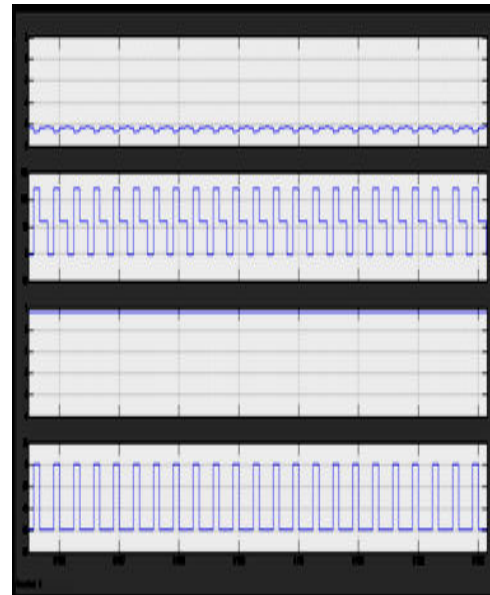

FIG 9 simulations of At IL1 and IL2 WAVE FORMS

FIG 10 simulations of Vd1 vd2 vd3 vd4 WAVE FORMS
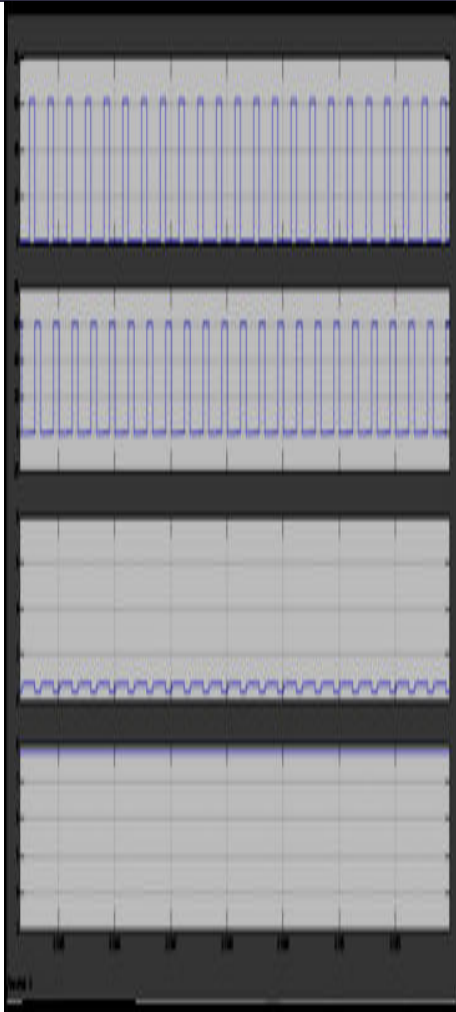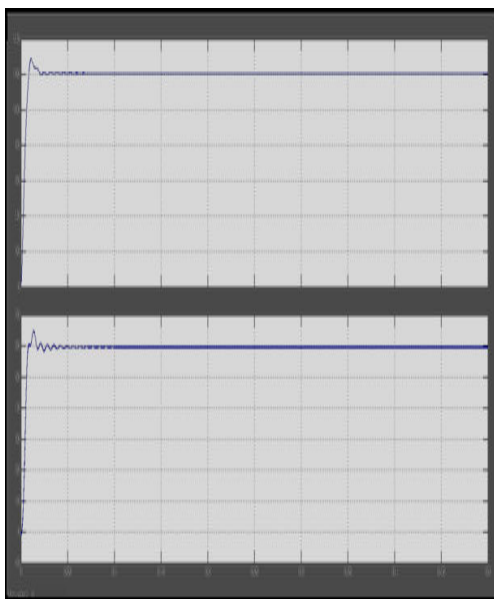
FIG 11 simulations of vs1 vs2 vs3 vs4
WAVE FORMS

Fig 12 simulations of V out and vc1
WAVE FORMs

Second operation state:
The load is supplied by PV,FC and Battery
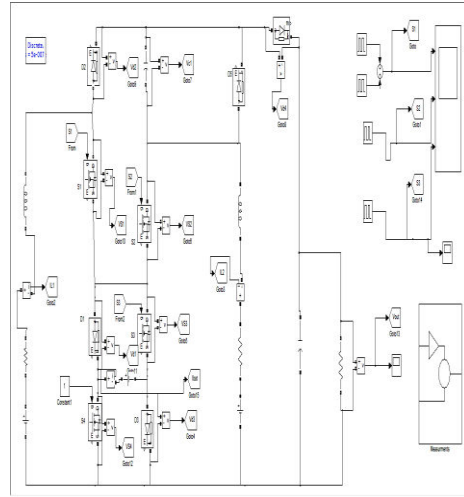
Fig 13 The load is supplied by PV,FC and
Battery Simulink diagram
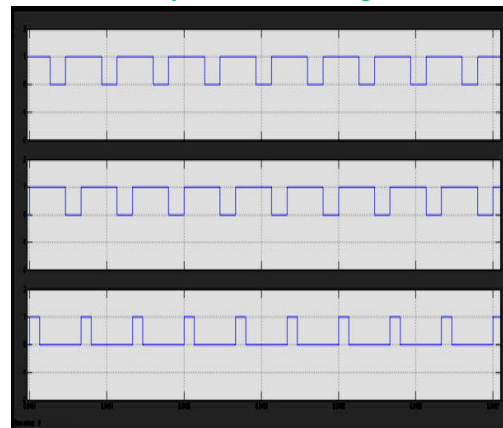
Fig 14 simulations ofSwitches s1 s2 s3
pulses

Fig 15simulations ofIL1 and IL2
charactersitics
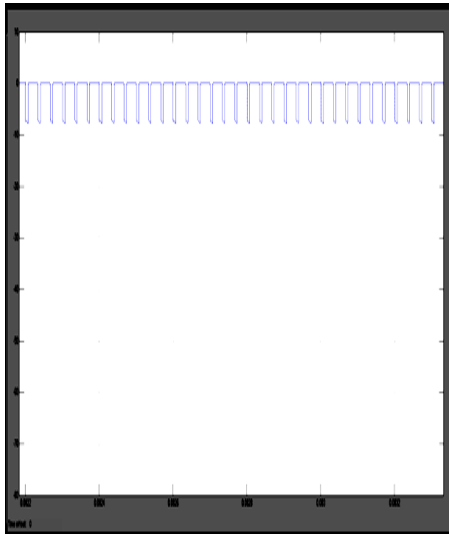
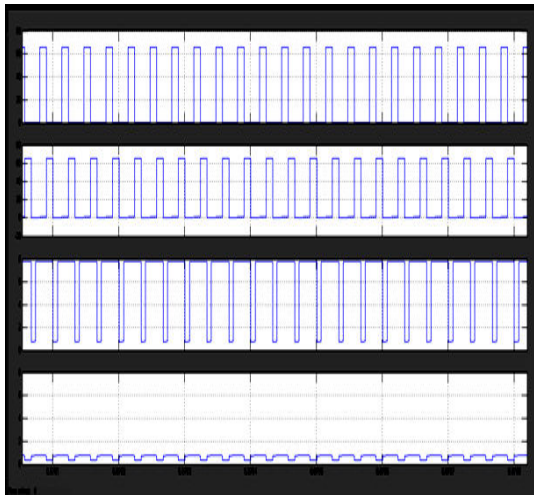Fig 16 simulations ofBattery current (ibat)

Fig 17simulations of Vs1 vs2 vs3 and vs4 waveforms

Fig 18 simulations of Vout wave forms

Fig 19 simulations of Vout and vcThird operation state
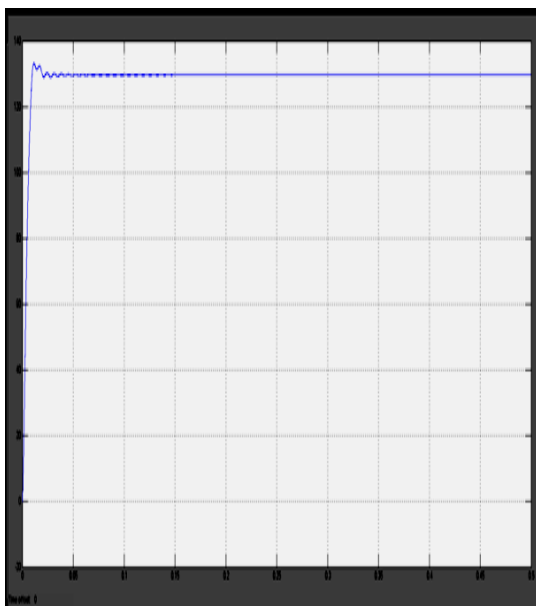

Fig 20 The load supplied by PV and FC while Battery is in charging mode
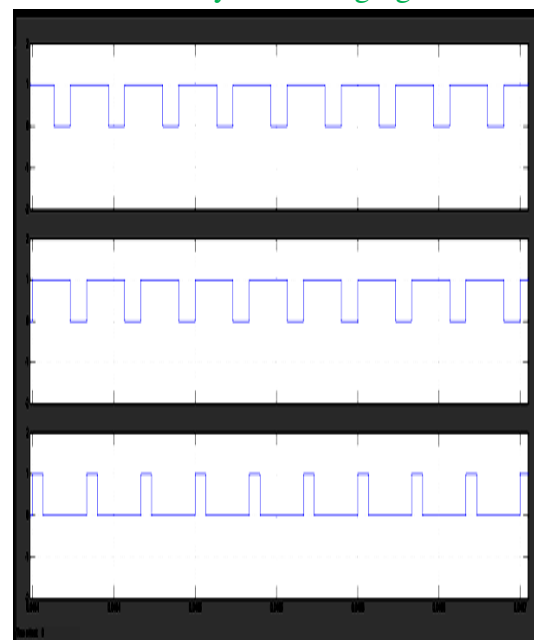

Fig 21 simulations of Switches s1 s2 s3 wave forms
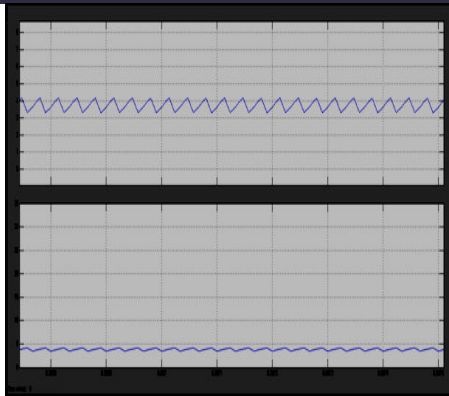
Fig 22 simulations of IL1 AND IL2 wave forms

Fig 23 simulations of Battery current waveforms

Fig 24 simulations of Vs1 vs2 vs3 vs4
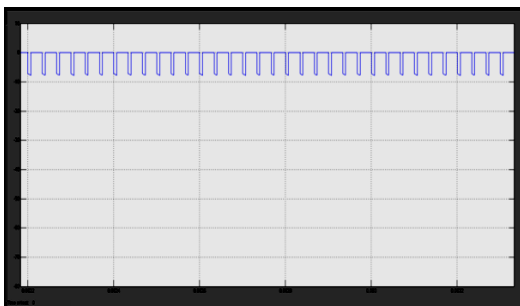

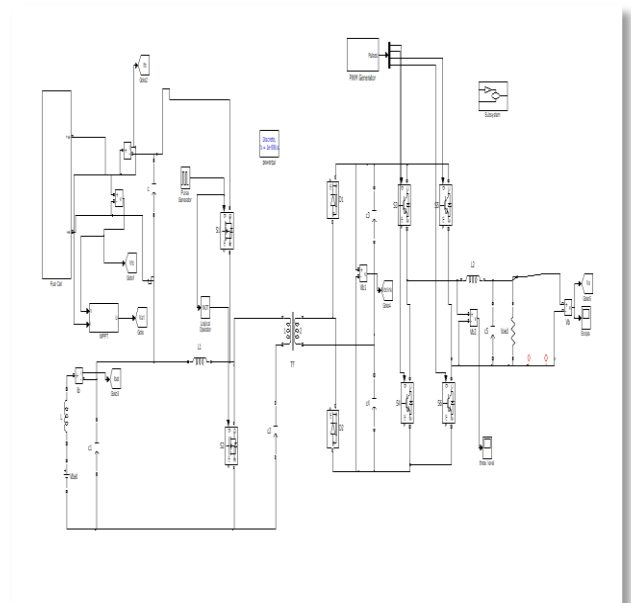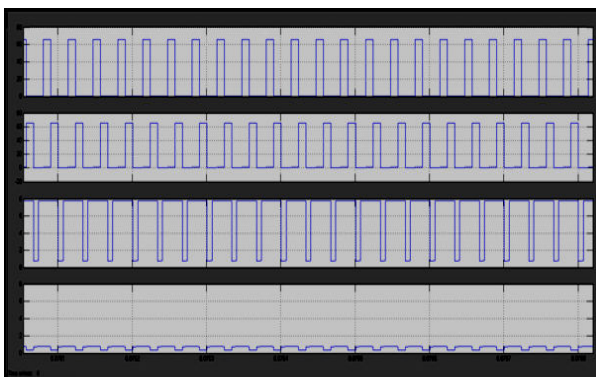Fig 25 simulations of Vc1 and vout
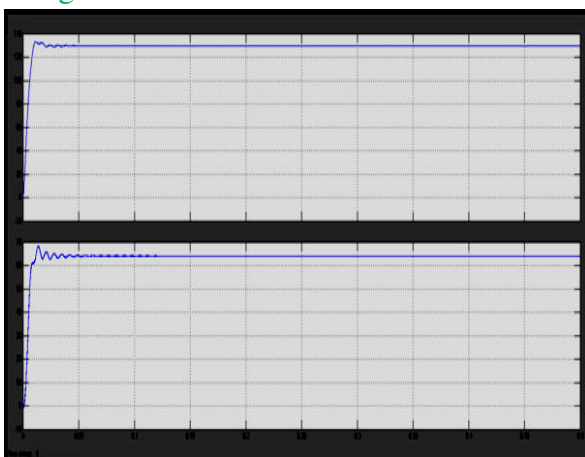

Fig 26 simulations of vout

Fig 27 simulink diagram of extension dc-dc converter
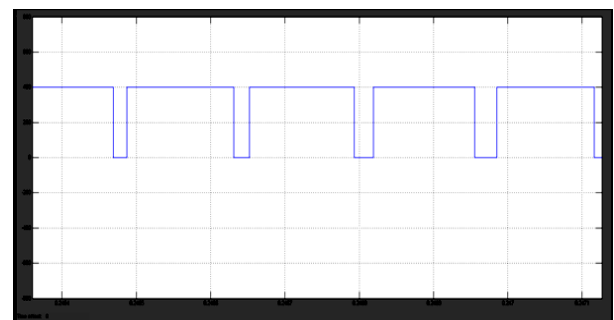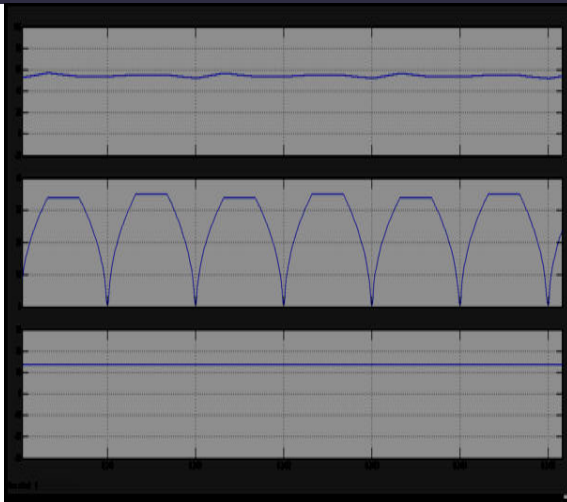

Fig 28simulations of Vb2 waveform

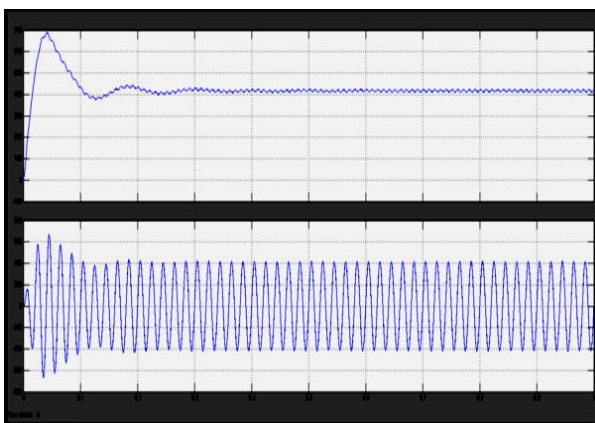Fig 29 simulations ofVoltage at fuel cell vfc currentifc and battery current ibat
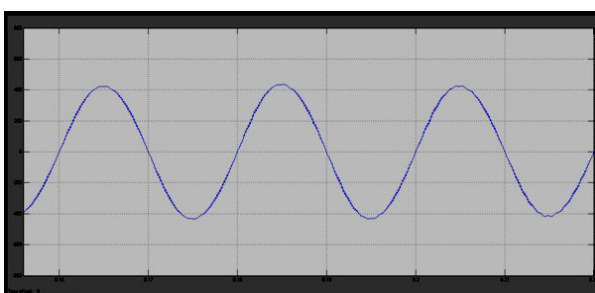

Fig 30 simulations ofVdclink vout

Fig 31 simulations of Vo sinusoidal waveform

V CONCLUSION

The multi input bidirectional DC-DC converter was designed to integrate more than two DC sources with different voltage levels which finds application in HEV. The multi input bidirectional converter can control the power flow between each pair of sources. The required voltage to drive a three phase induction motor is obtained by photo voltaic cells and multi input bidirectional DC-DC converter. MPPT control technique is used to extract the maximum power from solar irradiation. Instead of using individual converter in hybrid system using multi input bidirectional DC-DC converter is reduces the system size and cost. Therefore proposed converter provides the better efficiency but harmonics presents in voltage source. The performance of the system has been verified by simulation using MATLAB/SIMULINK environment.

REFERENCES

[1] A. Ostadi and M. Kazerani, "Optimal sizing of the battery unit in a plug-in electric vehicle," IEEE Trans. Veh. Technol., vol. 63, no. 7, pp. 3077–3084, Sep. 2014.

[2] P. Mulhall, S. M. Lukic, S. G. Wirashingha, Y.-J. Lee, and A. Emadi, "Solar-assisted electric auto rickshaw three-wheeler," IEEE Trans. Veh. Technol., vol. 59, no. 5, pp. 2298—2307, Jun. 2010.

[3] H. J. Chiu and L. W. Lin, "A bidirectional dc-dc converter for fuel cell electric vehicle driving system," IEEE Trans. Power Electron., vol. 21, no. 4, pp. 950–958, Jul. 2006.

[4] T. Markel, M. Zolot, K. B. Wipke, and A. A. Pesaran, "Energy storage requirements for hybrid fuel cell vehicles," presented at the Adv. Autom. Battery Conf., Nice, France, 2003.

[5] S. Miaosen, "Z-source inverter design, analysis, and its application in fuel cell vehicles," Ph.D. dissertation, Dept. Electr. Comput. Eng., Michigan State Univ., East Lansing, MI, USA, 2007.

[6] O. Hegazy, R. Barrero, J. Van Mierlo, P. Lataire, N. Omar, and T. Coosemans,

"An advanced power electronics interface for electric vehicles applications," IEEE Trans. Power Electron., vol. 28, no. 12, pp. 1–14, Dec. 2013.

[7] M. R. Feyzi, S. A. KH. Mozaffari Niapour, F. Nejabatkhah, S. Danyali, and A. Feizi, "Brushless DC motor drive based on multi-input DC boost converter supplemented hybrid PV/FC/Battery power system," in Proc. IEEE Electr. Comput. Eng. Conf., 2011, pp. 000442–000446.

[8] R. J. Wai, C. Y. Lin, and B. H. Chen, "High-efficiency DC–DC converter with two input power sources," IEEE Trans. Power Electron., vol. 27, no. 4, pp. 1862–1875, Apr. 2012.

[9] L. J. Chien, C. C. Chen, J. F. Chen, and Y. P. Hsieh, "Novel three-port converter with high-voltage gain," IEEE Trans. Power Electron., vol. 29, no. 9, pp. 4693–4703, Sep. 2014.

[10] R. B. Mohammad, H. Ardi, R. Alizadeh, and A. Farakhor, "Non-isolated multi-input–single-output DC/DC converter for photovoltaic power generation systems," IET Power Electron., vol. 7, no. 11, pp. 2806–2816, Jun. 2014.

[11] L. W. Zhou, B. X. Zhu, and Q. M. Luo, "High step-up converter with capacity of multiple input," IET Power Electron., vol. 5, no. 5, pp. 524–531, May 2012.

[12] A. Ajami, H. Ardi, and A. Farakhor, "A novel high step-up DC/DC converter based on integrating coupled inductor and switched-capacitor tech niques for renewable energy applications," IEEE Trans. Power Electron., vol. 30, no. 8, pp. 4255–4263, Aug. 2015.

[13] H. Ardi, R. R. Ahrabi, and S. N. Ravandanegh, "Non-isolated bidirectional DC–DC converter analysis and implementation," IET Power Electron., vol. 7, no. 12, pp. 3033–3044, Jun. 2014.

[14] R. Y. Duan and J. D. Lee, "High-efficiency bidirectional DC–DC converter with coupled inductor," IET Power Electron., vol. 5, no. 1, pp. 115–123, Jun. 2012.

[15] S. Danyali, S. H. Hosseini, and G. B. Gharehpetian, "New extendable single-stage multi-input DC–DC/AC boost converter," IEEE Trans. Power Electron., vol. 29, no. 2, pp. 775–788, Feb. 2014.

[16] L. Wang, Z. Wang, and H. Li, "Asymmetrical duty cycle control and de coupled power flow design of a three-port bidirectional DC-DC converter for fuel cell vehicle application," IEEE Trans. Power Electron., vol. 27, no. 2, pp. 891–904. Feb. 2012.

[17] S. Falcones, R. Ayyanar, and X. Mao, "A DC–DC multiport-converter based solid-state transformer integrating distributed generation and stor age," IEEE Trans. Power Electron., vol. 28, no. 5, pp. 2192—2203, May 2013.

[18] Y. M. Chen, A. Q. Huang, and X. Yu, "A high step-up three-port DC-DC converter for stand-alone PV/battery power systems," IEEE Trans. Power Electron., vol. 28, no. 11, pp. 5049–5062, Nov. 2013.

[19] K. Gummi and M. Ferdowsi, "Double-input DC–DC power electronic converters for electric-drive vehicles—Topology exploration and synthesis using a single-pole triple-throw switch," IEEE Trans. Ind. Electron., vol. 57, no. 2, pp. 617–623, Feb. 2010.

[20] R.-J. Wai, S.-J. Jhung, J.-J. Liaw, and Y.-R. Chang, "Intelligent optimal energy management system for hybrid power sources including fuel cell and battery," IEEE Trans. Power Electron., vol. 28, no. 7, pp. 3231–3244, Jul. 2013.

[21] S. Kelouwani, N. Henao, K. Agbossou, Y. Dube, and L. Boulon, "Two layer energy-management architecture for a fuel cell HEV using road trip information," IEEE Trans. Veh. Technol., vol. 61, no. 9, pp. 3851–3864, Nov. 2012.

[22] M. A. G. de Brito, L. Galotto, L. P. Sampaio, G. de Azevedo e Melo, and C. A. Canesin, "Evaluation of the main MPPT techniques for photovoltaic applications," IEEE Trans. Ind. Electron., vol. 60, no. 3, pp. 1156–1167, Mar. 2013.

[23] M. Koot, J. Kessels, B. de Jager, W. Heemels, P. Van den Bosch, and M. Steinbuch, "Energy management strategies for vehicular electric power systems," IEEE Trans. Veh. Technol., vol. 54, no. 3, pp. 771–782, May 2005.